Pak. J. Engg. & Appl. Sci. Vol. 14, Jan., 2014 (*p.* 38-56)

An Optimized Thermal Analysis of Electronic Unit Used in Aircraft

Asad Naeem Shah[1], Faisal Mir[1, *] and Muhammad Farooq[2]

1. Department of Mechanical Engineering, University of Engineering and Technology Lahore.
2. Department of Mechanical, Mechatronics & Manufacturing Engineering, KSK Campus, University of Engineering and Technology Lahore.

* Corresponding author; E-mail: engr.faisalmir@gmail.com

Abstract

In a field where change and growth is inevitable, new electronic packaging problems continuously arise. Smaller, but more powerful devices are prone to overheating causing intermittent system failures, corrupted signals and outright system failure. Current study is focused on the analysis of the optimized working of electronic equipment from thermal point of view. In order to achieve the objective, an approach was developed for the thermal analysis of Printed Circuit Board (PCB) including the heat dissipation of its electronic components and then removal of the heat in a sophisticated manner by considering the conduction and convection modes of heat transfer. Mathematical modeling was carried out for a certain problem to address the thermal design, and then a program was developed in MATLAB for the solution of model by using Newton-Raphson method. The proposed unit is to be mounted on an aircraft having suspected thermal characteristics owing to abrupt changes in pressure and temperature as aircraft moves quickly from a lower altitude to higher altitude. In current study, dominant mode of heat transfer was conduction revealing that the major portion of heat transfer takes place by copper cladding and that heat conduction along the length of PCB can be improved enormously by using even thin layer of copper. The results confirmed that temperatures of all the electronic components were within derated values. Meanwhile, it was known that convection also plays a significant role in the reduction of temperatures of the components. The reduction in nodal temperature was in the range of 13 to 42 %. Furthermore, altitude variation from sea level to 15240 m (above sea level) caused the reduction in pressure from 1atm to 0.1095 atm. Consequently, the temperature of the electronic components increased from 73.25^{o}C to 83.83^{o}C for first node 'a', and from 66.04^{o}C to 68.47^{o}C for last node 'n' because of the decrease in the convective heat transfer coefficient.

Key Words: Electronic equipment, Printed circuit board, Copper cladding, Heat transfer

1. Introduction

The efficient working of the electrical equipments/components is one of the major factors in the overall reliability and working of the electronic systems. It is imperative for all such components to operate properly as electric current passes through them. Heat is generated when current passes through these electric resistances. The continuous and relentless miniaturization of electronic devices has resulted in a massive increase in the heat generation per unit volume. These higher temperatures will damage electronic components and thus their safety and reliability will be adversely affected. It has been reported in literature that there is almost exponential increase in the rate of failure of electronic devices with the increase in operating temperature [1]. Further, it has also been elaborated that there is linear trend between the number of years and the number of components packed on a chip. It is important to note that when thousands or even millions of such components are packed in a small volume over the PCB, the heat generated increases to such a high level that its removal becomes a difficult task, and thus a major concern for the safety and reliability of the electronic equipments.

During the developing phase of electronic equipments used in aircraft, much attention is paid to the designing of circuit which is required to be

capable to accommodate as much electronic components on the PCB as are necessary for the desired function. Furthermore, effort is made to keep these components as close to each other as possible to get minimum signal losses during the working process. This results into the accumulation of power density hot spots and heat waves over the board which can cause failure in the operation of electronic equipment used in aircrafts. Therefore, it is imperative to remove such a heat surge at the populated electronic circuit board through the suitable thermal management techniques. Moreover, it is necessary to maintain the optimum distance conducive to transfer of the signals among the electronic components in order to minimize the effect of heat dissipation from one component to others.

Scientists are of the view that the components with high heat dissipation rate should be placed at the sides of the PCB and not in the middle of them so that a path of least thermal resistance may be achieved [1]. Lee et al. [2] analyzed a typical cellular phone. The interior of phone consisted of a single motherboard which was a PCB over which surface mount IC packages and other components were installed. The average gap provided between components and the case was approximately 1mm to 2 mm. In an effort by Ramakrishna, et al. [3], a three dimensional heat transfer problem was solved to determine the thermal and flow characteristics of a cellular phone. Simulation results predicted the external flow velocities as up to 0.2m/s, while internal flow velocities were negligibly small i.e. (0.02 m/s). The lack of any significant internal fluid motion indicated that the viscous forces were dominant due to the small gaps between the circuit board and the case walls, and thus heat was transferred mainly by the conduction.

The thermal conductivity of the PCB is the most important design parameter to reduce the board temperature. A marginal increase in the percentage of copper within the board results in the increase in effective thermal conductivity, and thus leads to a significant reduction in board temperature [4]. Thermal management of an environment power electronic system is another parameter to be considered. Thermal environment in this case is found to be between 65^{o}C and 90^{o}C which is considerably higher than many traditional electronics applications [5]. Similarly, convection also plays a significant role in the heat transfer among the components. For this, a modular, low cost and passive air cooling system is required. Eveloy et al. [6] discussed the suitability of heat transfer in free convection conditions using CFD analysis, and thus predicted the multi-component PCB heat transfer. It has also been established that increase in chip spacing decreases the thermal resistance of the circuit board for various cooling configurations only if accompanied by an increased board thickness [7]. In addition, the analytical solution had also been used to estimate the accuracy of the compound-fin model for one-dimensional steady heat conduction in a microelectronic circuit board. Sarvar et al. [8] presented an approach for the semiconductor package design incorporating the integrated air cooled heat sinks for a power converter. The model developed in this research was helpful to increase the life of electronic devices as it would be equally important to design the product from thermal point of view. Further, the research could be utilized to increase the market value of the product by increasing its reliability through proper thermal design.

PCBs are primarily an insulating material used as base, into which conductive strips are printed. The base material is generally fiber glass (FR-4), and the conductive connections/planes are of generally copper and are made through an etching process. Copper cladding is commonly used to enhance the current carrying capacity and heat conduction along the PCBs. The thickness of copper cladding on the PCB is usually expressed in terms of ounce of copper which is the thickness of 1 ft^2 copper sheet. One ounce of copper is equivalent to 0.035mm (1.4mil) thickness of a copper layer.

The objective of research is to evaluate thermal behavior of an electronic unit used in aircraft and then to investigate whether the design meets the specific thermal requirements with optimum electronic needs. This work presents a very easy approach for the physical interpretation of the problem in hand. First of all, the unit is analyzed by varying the thermal conductivity of the PCB and thus thermal effects are examined. Input data for the electronic components, heat dissipation and size

details are available in the manufacturer's data sheets shown in Annexure-I. The performance of the electronic unit is then analyzed by considering different modes of heat transfer to investigate the working of the components with in their operating temperature ranges. Meanwhile, the effect of pressure variation due to change in altitude on thermal performance is also addressed. Although some research work has already been reported on this issue, the present research will provide the analytical approach to solve the specific problem by using finite difference method in which Newton-Raphson method is utilized to solve the non linear equations.

2. Process Description and Mathematical Modeling

In order to perform thermal analysis, a PCB with following inputs is considered:

Table 1 Parameters of PCB

Parameter	Symbol	Value
Length of PCB	L	144 mm
Width of PCB	w	106 mm
Thickness of PCB	t	1.6 mm
No of Cu layers in PCB		1 layer of 2 layer PCB and 4 layers for multi layer PCB
Percentage of Cu in PCB		Variable

Investigation is made for considering six different cases for PCBs in which the thickness of copper layer (copper cladding), percentage area coverage of copper and effective conductivities of PCB are varied by keeping the thickness of the PCB as constant and using formula Eqn (1).

$$Q_{FCB} = Q_{FR..4} + Q_{Cu}$$

$$= \frac{[(kA)_{FR.4} + (kA)_{Cu}]\Delta T}{L} \qquad (1)$$

where

- w = width of PCB
- t = total thickness of PCB
- k_{FR-4} = thermal conductivity of FR-4
- k_{Cu} = thermal conductivity of copper
- t_{FR-4} = thickness of FR-4
- t_{Cu} = thickness of copper layer

Here are 6 different cases to find effective thermal conductivity of 2 layer and 4 layer PCB. The results are listed in Table 2 & 3 respectively.

Table 2 Effective Thermal Conductivities of 2 Layers PCB

Case – 1

%age Coverage	Thickness of Cu (mm) (Top & Bottom)	Effective K of PCB (W/mK)	%age of conduction due to copper layer
20	0.07	3.666125	91.89
30	0.07	5.3491875	94.47
40	0.07	7.03225	95.81
50	0.07	8.7153125	96.63
60	0.07	10.398375	97.19
70	0.07	12.0814375	97.59
80	0.07	13.7645	97.90
90	0.07	15.4475625	98.13

Case – 2

%age Coverage	Thickness of Cu (mm) (Top & Bottom)	Effective K of PCB (W/mK)	%age of conduction due to copper layer
20	0.14	7.03225	95.81
30	0.14	10.398375	97.19
40	0.14	13.7645	97.90
50	0.14	17.130625	98.33
60	0.14	20.49675	98.61
70	0.14	23.862875	98.82
80	0.14	27.229	98.98
90	0.14	30.595125	99.10

Case – 3

%age Coverage	Thickness of Cu (mm) (Top & Bottom)	Effective K of PCB (W/mK)	%age of conduction due to copper layer
20	0.21	10.398375	97.19
30	0.21	15.4475625	98.13
40	0.21	20.49675	98.61
50	0.21	25.5459375	98.90
60	0.21	30.595125	99.10
70	0.21	35.6443125	99.24
80	0.21	40.6935	99.34
90	0.21	45.7426875	99.42

Table 3 Effective Thermal Conductivities of Multilayer PCB

Name of Layers	Thickness (Micron)	Conductor Material	Coverage (%)	Effective K of PCB (W/mK)
Case – 4				
Signal	70	Copper	20	22.179813
Power or Ground	35	Copper	90	
Power or Ground	35	Copper	90	
Signal	70	Copper (Pure)	20	
Case – 5				
Signal	70	Copper	50	32.278188
Power or Ground	35	Copper	90	
Power or Ground	35	Copper	90	
Signal	70	Copper (Pure)	50	
Case – 6				
Signal	70	Copper	80	42.37656
Power or Ground	35	Copper	90	
Power or Ground	35	Copper	90	
Signal	70	Copper (Pure)	80	

2.1 Heat Dissipation of Electronic Components

The heat dissipations of electronic components are obtained from the components manufacturer data sheets. Generally it is welknown that power is voltage times current. Actually, this power is the heat dissipation if there is no output from the system. In case of a system with inputs and outputs, the heat dissipation is the difference between the power entering and leaving [9]. Moreover, it has been observed through experience that most of the electronic systems are 75-85% efficient so heat dissipation is considered between 15-25% of total input power. Table 4 shows the values of heat dissipation of electronic components at nodes with 20% of total input powers. These nodal heat dissipation values will be used further for thermal analysis.

Table 4 Heat dissipation (Q) of electronic components at various nodes

Heat Dissipation	Watt
Q_a	**3.36**
Q_b	**3.36**
Q_c	**0.576**
Q_d	**0.8**
Q_e	**3.36**
Q_f	**3.36**
Q_g	**0.38**
Q_h	**0.8**
Q_i	**0**
Q_j	**0.2028**
Q_k	**0.192**
Q_l	**0.8**
Q_m	**0.166**
Q_n	**0.8**

2.2 Heat Flow Model

A typical thermal model is a finite difference thermal model which is a discretized mathematical representation of the system to be simulated. The thermal analysis is performed by using the heat balance equation $Q_{in} = Q_{out}$ to obtain the componenets temperatures. Following assumptions are also made during the analysis:

All the heat is flowing into the node. Components having least heat dissipation values 0.1 W are not considered. Components are positioned so that they are aligned in the form of rows and columns. Dummy nodes are considered where it is necessary. Heat is leaving PCB from only two ends where fasteners are attached. Cross sectional area specified for one row or column does not overlap the area specified for others.

Above mentioned design alterations cause no effect on the thermal analysis of the electronic equipment. The model of electronic equipment consists of a PCB and electronic components mounted on it as shown in Fig.1 (a)-(f). The details are as follows:

The PCB and electronic components are divided into different parts shown in Fig.1 (d). Electronic components are represented by nodes from ‘a’ to ‘n’ as depicted in Fig.1 (e). Q_a to Q_n are nodal heat dissipations as revealed in Table 4. The thermal resistance network is developed by showing

conductance among nodes from $K_{1\text{-}27}$ as shown in Fig.1 (f).

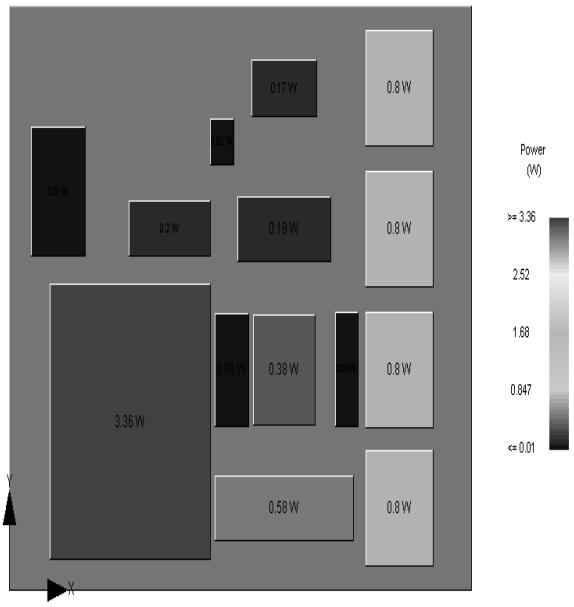

1(a)

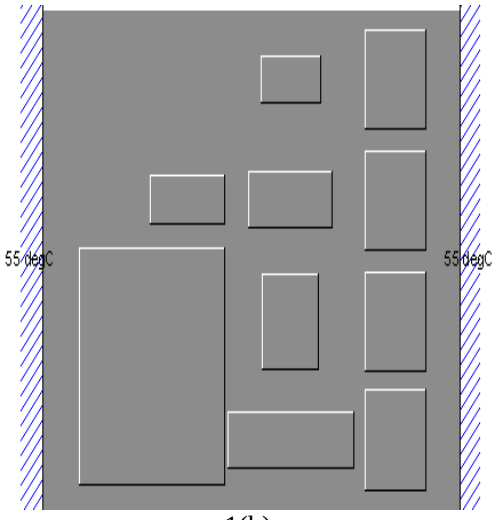

1(b)

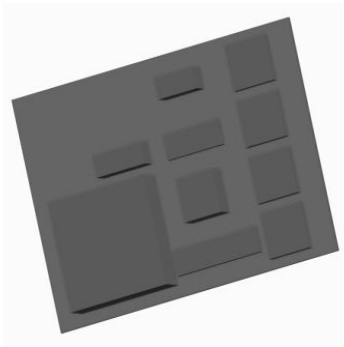

1(c)

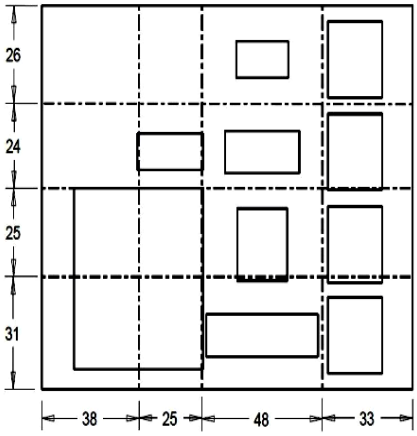

1(d)

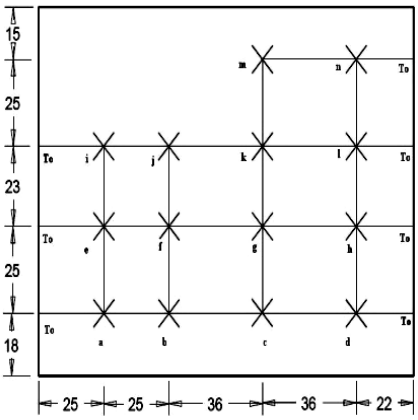

1(e)

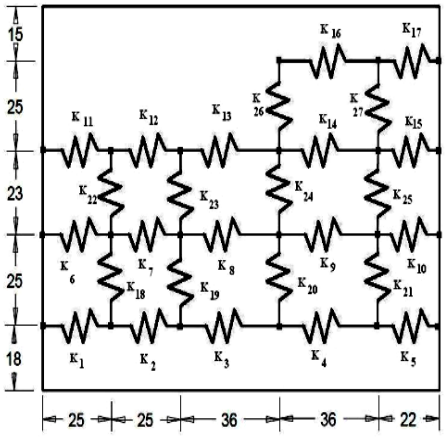

1(f)

Fig.1 (a) Electronic equipment & components colored by heat dissipations, 1(b) Modeling level, 1(c) Electronic equipment 3-D view, 1(d) represents the area distribution of the equipment, 1(e) nodal distribution and node to node distances,1(f) thermal resistance network model.

Now thermal conductance can be calculated by considering the Eqn (2):

$$K = k_{eff} A / L \quad (2)$$

where

k_{eff} = Effective thermal conductivity of PCB
K = Thermal conductance

Eqn (2) can be used for the calculation of various conductances K_1, K_2 …K_{27} by considering the thickness of PCB, corresponding width of area distribution and node to node distance. Its solution is given in Table 5.

Table 5 Values of conductance for the different cases of effective thermal conductivities

Conductance of Electronic Equipment		**Case 1**	**Case 2**	**Case 3**	**Case 4**	**Case 5**	**Case 6**
Sr. No	**Conductance Name**	**Conductance (W/K)**	**Conductance (W/K)**	**Conductance (W/K)**	**Conductance (W/K)**	**Conductance (W/K)**	**Conductance (W/K)**
1	**K_1**	0.0073	0.0173	0.0306	0.0438	0.0639	0.0839
2	**K_2**	0.0073	0.0173	0.0306	0.0438	0.0639	0.0839
3	**K_3**	0.0051	0.0120	0.0212	0.0304	0.0444	0.0583
4	**K_4**	0.0051	0.0120	0.0212	0.0304	0.0444	0.0583
5	**K_5**	0.0083	0.0196	0.0347	0.0498	0.0726	0.0954
6	**K_6**	0.0059	0.0139	0.0246	0.0354	0.0515	0.0677
7	**K_7**	0.0059	0.0139	0.0246	0.0354	0.0515	0.0677
8	**K_8**	0.0041	0.0097	0.0171	0.0246	0.0358	0.0470
9	**K_9**	0.0041	0.0097	0.0171	0.0246	0.0358	0.0470
10	**K_{10}**	0.0067	0.0158	0.0280	0.0402	0.0585	0.0769
11	**K_{11}**	0.0056	0.0134	0.0237	0.0339	0.0495	0.0650
12	**K_{12}**	0.0056	0.0134	0.0237	0.0339	0.0495	0.0650
13	**K_{13}**	0.0039	0.0093	0.0164	0.0236	0.0343	0.0451
14	**K_{14}**	0.0039	0.0093	0.0164	0.0236	0.0343	0.0451
15	**K_{15}**	0.0064	0.0152	0.0269	0.0386	0.0562	0.0738
16	**K_{16}**	0.0042	0.0101	0.0178	0.0255	0.0372	0.0489
17	**K_{17}**	0.0069	0.0165	0.0291	0.0418	0.0609	0.0800
18	**K_{18}**	0.0089	0.0212	0.0375	0.0537	0.0783	0.1029
19	**K_{19}**	0.0059	0.0139	0.0246	0.0354	0.0515	0.0677
20	**K_{20}**	0.0113	0.0267	0.0473	0.0679	0.0989	0.1299
21	**K_{21}**	0.0077	0.0184	0.0325	0.0467	0.0680	0.0893
22	**K_{22}**	0.0097	0.0230	0.0407	0.0584	0.0851	0.1118
23	**K_{23}**	0.0064	0.0151	0.0268	0.0384	0.0560	0.0736
24	**K_{24}**	0.0122	0.0291	0.0514	0.0738	0.1075	0.1412
25	**K_{25}**	0.0084	0.0200	0.0354	0.0507	0.0739	0.0971
26	**K_{26}**	0.0113	0.0267	0.0473	0.0679	0.0989	0.1299
27	**K_{27}**	0.0077	0.0184	0.0325	0.0467	0.0680	0.0893

2.3 Heat Flow Balance Equation of Each Node for Conduction

After finding the conductance in Table 5, a system of the heat flow balance equations is developed for each node using the Eqn. (1) and following the assumptions:

Heat conduction is along the length of the PCB due to the fact that heat transfer takes place only through the ends where wedge lock screws are attached. Thermal properties of the board are constant. Steady state heat transfer is considered. Temperature of sink is considered to be 55°C (worst hot case). The electronic components, with less than 0.1 W heat dissipation are not considered in the solution.

$$\left.\begin{aligned}
&\text{For Node "a" } K_1(T_o-T_a)+K_2(T_b-T_a)+K_{18}(T_e-T_a)+Q_a=0\\
&\text{For Node "b" } K_2(T_a-T_b)+K_3(T_c-T_b)+K_{19}(T_f-T_b)+Q_b=0\\
&\text{For Node "c" } K_3(T_b-T_c)+K_4(T_d-T_c)+K_{20}(T_g-T_c)+Q_c=0\\
&\text{For Node "d" } K_4(T_c-T_d)+K_5(T_o-T_d)+K_{21}(T_h-T_d)+Q_d=0\\
&\text{For Node "e" } K_6(T_o-T_e)+K_{18}(T_a-T_e)+K_7(T_f-T_e)+K_{22}(T_i-T_e)+Q_e=0\\
&\text{For Node "f" } K_7(T_e-T_f)+K_8(T_g-T_f)+K_{19}(T_b-T_f)+K_{23}(T_j-T_f)+Q_f=0\\
&\text{For Node "g" } K_8(T_f-T_g)+K_9(T_h-T_g)+K_{20}(T_c-T_g)+K_{24}(T_k-T_g)+Q_g=0\\
&\text{For Node "h" } K_9(T_g-T_h)+K_{10}(T_o-T_h)+K_{21}(T_d-T_h)+K_{25}(T_l-T_h)+Q_h=0\\
&\text{For Node "i" } K_{11}(T_o-T_i)+K_{12}(T_j-T_i)+K_{22}(T_e-T_i)+Q_i=0\\
&\text{For Node "j" } K_{13}(T_i-T_j)+K_{13}(T_k-T_j)+K_{23}(T_f-T_j)+Q_j=0\\
&\text{For Node "k" } K_{13}(T_j-T_k)+K_{14}(T_l-T_k)+K_{24}(T_g-T_k)+K_{26}(T_m-T_k)+Q_k=0\\
&\text{For Node "l" } K_{14}(T_k-T_l)+K_{15}(T_o-T_l)+K_{25}(T_h-T_l)+K_{27}(T_n-T_l)+Q_l=0\\
&\text{For Node "m" } K_{26}(T_k-T_m)+K_{16}(T_n-T_m)+Q_m=0\\
&\text{For Node "n" } K_{16}(T_m-T_n)+K_{17}(T_o-T_n)+K_{27}(T_l-T_n)+Q_n=0
\end{aligned}\right\} \quad (3)$$

2.2 Heat Transfer through Convection

The convection mode of heat transfer can be considered for the analysis using the Newton's law of cooling [1].

$$q = h A_s (T_s - T_{smb}) \quad (4)$$

where

- q = Convective heat transfer
- A_s = Surface area
- h = Convective heat transfer coefficient
- T_s = Surface temperature
- T = System temperature

When electronic components are placed on the PCB used in aircraft, natural heat transfer coefficient is found from the empirical relation given in [1]:

$$q = 2.44A(P)^{0.5}(\Delta T)^{1.25} \Big/ (L)^{1.25} \quad (5)$$

where

- q = Characteristic length in meter
- A_s = Atmospheric pressure

$$\Delta T = T_s - T_{smb}$$

The electronic equipment in the present case is placed vertically in the space allocated in the aircraft as per requirement of allocation and compactness of space. Due to convection effect another resistance is added in the analysis and thus mathematical model is changed accordingly [10]. Thus the refined heat flow balance equations model including the convection effect is derived on the basis of previous assumptions:

System temperature is 65°C and radiation effect is neglected owing to its negligible contribution in the cooling of equipment in the present case.

$$\left.\begin{aligned}
&\text{For Node "a" } K_1(T_o-T_a)+K_2(T_b-T_a)+K_{18}(T_e-T_a)+Q_a+q_a=0\\
&\text{Where } q_a = 2.44(A)(P)^{0.5}\frac{(T_{am}-T_a)^{2.25}}{(L)^{0.25}}\\
&\text{For Node "b" } K_2(T_a-T_b)+K_3(T_c-T_b)+K_{19}(T_f-T_b)+Q_b+q_b=0\\
&\text{Where } q_b = 2.44(A)(P)^{0.5}\frac{(T_{am}-T_b)^{2.25}}{(L)^{0.25}}
\end{aligned}\right\} \quad (6)$$

(Eqn 6 continued)

For Node "c" $K_3(T_b–T_c)+K_4(T_d–T_c) + K_{20}(T_g–T_c) + Q_c + q_c = 0$

Where $q_c = 2.44(A)(P)^{0.5}\frac{(T_{am}–T_c)^{2.25}}{(L)^{0.25}}$

For Node "d" $K_4(T_c–T_d)+K_5(T_o–T_d) + K_{21}(T_h–T_d) + Q_d + q_d = 0$

Where $q_d = 2.44(A)(P)^{0.5}\frac{(T_{am}–T_d)^{2.25}}{(L)^{0.25}}$

For Node "e" $K_6(T_o–T_e)+K_{18}(T_a–T_e) + K_7(T_f–T_e) +K_{22}(T_i–T_e) + Q_e + q_e = 0$

Where $q_e = 2.44(A)(P)^{0.5}\frac{(T_{am}–T_e)^{2.25}}{(L)^{0.25}}$

For Node "f" $K_7(T_e–T_f)+K_8(T_g–T_f) + K_{19}(T_b–T_f) +K_{23}(T_j–T_f) + Q_f + q_f = 0$

Where $q_f = 2.44(A)(P)^{0.5}\frac{(T_{am}–T_f)^{2.25}}{(L)^{0.25}}$

For Node "g" $K_8(T_f–T_g)+K_9(T_h–T_g) + K_{20}(T_c–T_g) +K_{24}(T_k–T_g) + Q_g + q_g = 0$

Where $q_g = 2.44(A)(P)^{0.5}\frac{(T_{am}–T_g)^{2.25}}{(L)^{0.25}}$

For Node "h" $K_9(T_g–T_h)+K_{10}(T_o–T_h) + K_{21}(T_d–T_h) +K_{25}(T_l–T_h) + q_h = 0$

Where $q_h = 2.44(A)(P)^{0.5}\frac{(T_{am}–T_h)^{2.25}}{(L)^{0.25}}$

For Node "i" $K_{11}(T_o–T_i)+K_{12}(T_j–T_i) + K_{22}(T_e–T_i) + Q_i + q_i = 0$

Where $q_i = 2.44(A)(P)^{0.5}\frac{(T_{am}–T_i)^{2.25}}{(L)^{0.25}}$

For Node "j" $K_{13}(T_i–T_j)+K_{13}(T_k–T_j) + K_{23}(T_f–T_j) + Q_j + q_j = 0$

Where $q_j = 2.44(A)(P)^{0.5}\frac{(T_{am}–T_j)^{2.25}}{(L)^{0.25}}$

For Node "k" $K_{13}(T_j–T_k)+K_{14}(T_l–T_k) +K_{24}(T_g–T_k) +K_{26}(T_m–T_k) + Q_k = 0$

Where $q_k = 2.44(A)(P)^{0.5}\frac{(T_{am}–T_k)^{2.25}}{(L)^{0.25}}$

For Node "l" $K_{14}(T_k–T_l)+K_{15}(T_o–T_l) + K_{25}(T_h–T_l) +K_{27}(T_n–T_l) + Q_l + q_l = 0$

Where $q_l = 2.44(A)(P)^{0.5}\frac{(T_{am}–T_l)^{2.25}}{(L)^{0.25}}$

For Node "m" $K_{26}(T_k–T_m)+K_{16}(T_n–T_m) + Q_m + q_m = 0$

Where $q_m = 2.44(A)(P)^{0.5}\frac{(T_{am}–T_m)^{2.25}}{(L)^{0.25}}$

For Node "n" $K_{16}(T_m–T_n)+K_{17}(T_o–T_n) + K_{27}(T_l–T_n) + Q_n + q_n = 0$

Where $q_n = 2.44(A)(P)^{0.5}\frac{(T_{am}–T_n)^{2.25}}{(L)^{0.25}}$

(6)

Table 6 Comparison of conduction cases of electronic equipment

Node	Case 6 Temperature. (^oC)	Case 5 Temperature (^oC)	Case 4 Temperature (^oC)	Case 3 Temperature (^oC)	Case 2 Temperature (^oC)	Case 1 Temperature (^oC)	Operating Temperature Range (^oC)
Ta	110.36	127.72	160.96	113.45	324.16	693.73	(-40 ~ 105)
Tb	130.09	153.64	198.72	117.16	420.07	921.34	(-40 ~ 105)
Tc	105.90	121.87	152.43	120.51	302.49	642.30	(-55 ~ 125)
Td	79.27	86.88	101.45	121.66	173.00	335.02	(-25 ~ 125)
Te	106.76	123.00	154.08	157.34	306.68	652.26	(-40 ~ 105)
Tf	125.73	147.91	190.37	160.10	398.88	871.05	(-40 ~ 105)
Tg	102.57	117.49	146.04	170.35	286.27	603.82	(-55 ~ 125)
Th	78.85	86.33	100.65	185.65	170.95	330.16	(-25 ~ 125)
Ti	93.26	105.26	128.23	194.81	241.03	496.47	Dummy
Tj	108.29	125.00	156.99	197.18	314.09	669.83	(-60 ~ 150)
Tk	96.99	110.17	135.38	201.37	259.17	539.52	(-55 ~ 125)
Tl	77.63	84.73	98.32	207.06	165.04	316.12	(-25 ~ 125)
Tm	92.26	103.95	126.32	249.27	236.16	484.90	(-25 ~ 95)
Tn	76.28	82.95	95.73	261.24	158.46	300.52	(-25 ~ 125)
Grand Total	1384.231765	1576.894523	1945.656273	2457.143093	3756.4372	7857.047943	

3. Solution of Equations

The heat flow balance equations of each node from system Eqn (6) are solved by generating MATLAB code and considering the case 6 of conduction as the initial values. It is clear when convective effect is taken into account the system equations are not linear now. In order to solve this problem iterative method is required [11]. Newton-Raphson method is employed in this analysis for the solution of heat flow balance equations. The basic equation of Newton-Raphson Method is as follows [12]:

$$X_{n+1} = X_n - f(X_n)/d)f(X_n) \qquad (7)$$

where

X = variable

Now solution of system of Eqn (6) using Newton-Raphson Method is given in Table 7.

Moreover, the effect of variation in pressure on previously discussed mode of heat transfer is presented in Table 8.

4. Results and Discussion

4.1 Effect of copper cladding on PCB conductivity

Fig. 2 presents that even a thin layer of copper cladding (in microns) can largely improve the heat conduction along the PCB. It also shows the trend of percentage heat conduction along the PCB due to copper layers in 2-layer PCBs. It is noteworthy that a large amount of heat is conducted on account of slight increase in copper (even in microns) and only negligible amount of heat is conducted due to FR-4 PCB dielectric material. These results are in consistent to the finding of Culham et al. [4] that the thermal conductivity of the PCB is the sole important design parameter for reducing temperature of electronic components placed over PCB.

4.2 Effect of Conduction on Electronic equipment

Fig. 3 presents the comparison of the 6 cases showing nodal temperatures for various nodes. It is clear that significant reduction in nodal temperature takes place with the increase in conductivity of the PCBs. This is one of the techniques of thermal management which is utilized to keep the electronic components temperatures within de-rating values. The results show that the approach by which heat transfer takes place through conduction, has brought quite obvious reduction in the nodal temperatures (components temperature) from node 'a' to 'n' from case 1 to 6 respectively. However, the most efficient case i.e. case 6 evidently indicates that some nodal temperatures are still out of the operating temperature range. This shows that some other methods should be

adopted in the thermal management of electronic equipment in order to keep the components temperatures within the range. Furthermore, it is also due to the fact that only conduction is considered in this thermal analysis which is contrary to the fact that convection also plays an important role in the thermal analysis of electronic equipments used in aircrafts.

4.3 Effect of Convection on Electronic equipment

In this case, natural convection mode of heat transfer is used for the case no. 6 which was the most efficient case of heat transfer during conduction. Fig. 4 shows the node wise comparisons of temperatures. It has been noted that the nodal temperatures are reduced and solution become converged for case no. 7. It also confirms that tempearture of all the nodes are within the opearting temperature ranges. The results indicate that convection also plays an important role in the heat tranfer of electronic equipments used in the aircrafts.

4.4 Effect of Pressure Variation

The effect of variation in pressure is also considered in this analysis as the electronic equipment is to operate at different altitudes above sea level. It is apparent from Fig. 5 that with the increase in altitude the heat transfer due to convection decreases and the conduction plays an important role to remove heat from the equipment and keep the temperatures with in operating range. It is due to the fact that the decrease in pressure results into decrease in convective heat transfer coefficient. It is important to note that total change in temperature per cycle remains below 20^{o}C for each node during the change in pressure from atmospheric condition to that at a height over 50,000ft i.e. during the total flight cycle. Moreover, Fig. 6 validates that the equipment is safe to operate in the said pressure and altitude ranges which is also recommended by the IPC. This is one of the important factors from the reliability point of view for electronic equipment.

Table 7 Solution of system of eqn (6) for temperature (°C)

Node	Iteration 1	Iteration 2	Iteration 3	Iteration 4	Iteration 5	Iteration 6
$\mathbf{T_a}$	110.36	77.85	73.45	73.25	73.25	73.25
$\mathbf{T_b}$	130.09	81.98	74.77	74.33	74.32	74.32
$\mathbf{T_c}$	105.90	73.91	68.05	67.30	67.27	67.27
$\mathbf{T_d}$	79.27	68.37	66.53	66.37	66.36	66.36
$\mathbf{T_e}$	106.76	77.80	74.26	74.14	74.14	74.14
$\mathbf{T_f}$	125.73	81.65	75.43	75.12	75.11	75.11
$\mathbf{T_g}$	102.57	75.73	72.15	72.00	72.00	72.00
$\mathbf{T_h}$	78.85	68.40	66.72	66.59	66.59	66.59
$\mathbf{T_i}$	93.26	93.26	93.26	93.26	93.26	93.26
$\mathbf{T_j}$	108.29	75.86	70.77	70.41	70.41	70.41
$\mathbf{T_k}$	96.99	72.66	68.63	68.29	68.28	68.28
$\mathbf{T_l}$	77.63	68.37	66.97	66.89	66.89	66.89
$\mathbf{T_m}$	92.26	72.23	69.29	69.13	69.12	69.12
$\mathbf{T_n}$	76.28	67.64	66.18	66.04	66.04	66.04

Table 8 Nodal temperatures at different pressures and altitudes

	P =1 atm	P=0.785 atm	P=0.609 atm	P=0.564 atm	P=0.297 atm	P=0.1095 atm			
Node temperature	**At sea level**	**2000 m above sea level**	**4000 m above sea level**	**4572 m above sea level**	**9144 m above sea level**	**15240 m above sea level**	**(ΔT) Change in Temperature per cycle (^{o}C)**	**Recommended IPC (ΔT) change in temperature per cycle**	**Operating temperature range (^{o}C)**
T_a	73.25	73.95	74.76	75.02	77.71	83.83	10.58	20.00	-40~ 105
T_b	74.32	75.15	76.12	76.44	80.01	89.00	14.67	20.00	-40~ 105
T_c	67.27	67.50	67.81	67.93	69.79	75.85	8.58	20.00	-55~ 125
T_d	66.36	66.49	66.65	66.70	67.41	69.44	3.08	20.00	-25~ 125
T_e	74.14	74.89	75.73	76.00	78.63	84.16	10.02	20.00	-40~ 105
T_f	75.11	75.99	77.00	77.33	80.83	89.09	13.98	20.00	-40~ 105
T_g	72.00	72.59	73.26	73.48	75.72	80.74	8.74	20.00	-55~ 125
T_h	66.59	66.74	66.91	66.97	67.69	69.63	3.04	20.00	-25~ 125
T_i	93.26	93.26	93.26	93.26	93.26	93.26	0.00	20.00	Dummy
T_j	70.41	70.90	71.48	71.68	73.96	80.00	9.60	20.00	-60~ 150
T_k	68.28	68.59	68.96	69.09	70.69	75.23	6.95	20.00	-55~ 125
T_l	66.89	67.06	67.27	67.33	68.10	70.03	3.15	20.00	-25~ 125
T_m	69.12	69.49	69.91	70.05	71.57	75.32	6.19	20.00	-25~ 95
T_n	66.04	66.14	66.26	66.30	66.85	68.47	2.43	20.00	-25~ 125

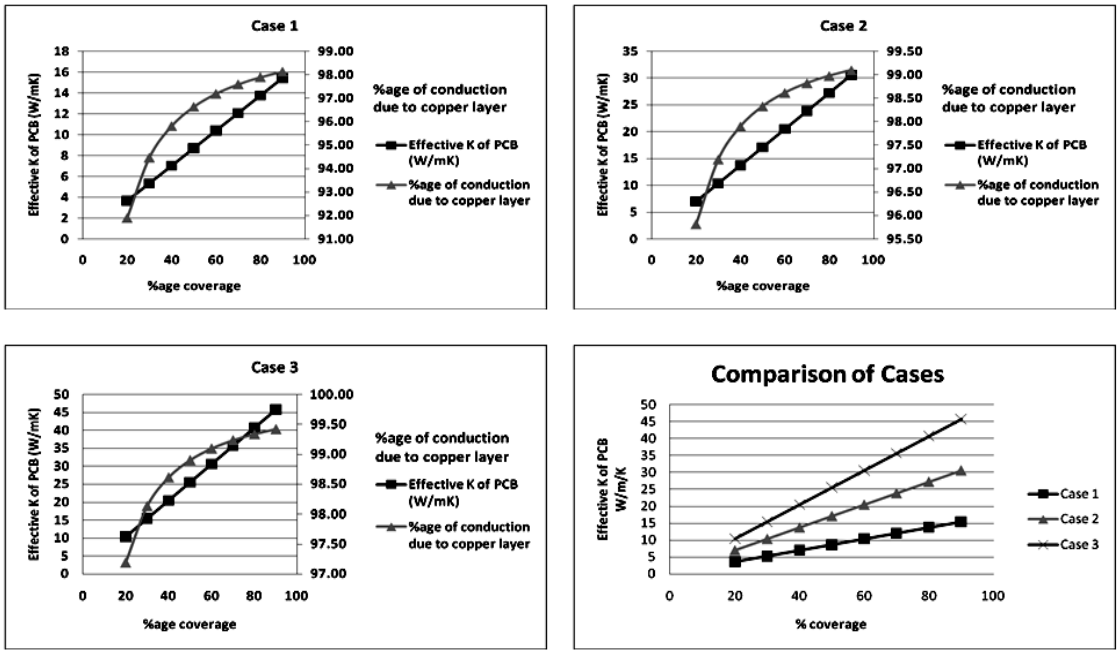

Fig. 2 Effective conductivity of PCB & Percentage of heat conduction due to copper layers

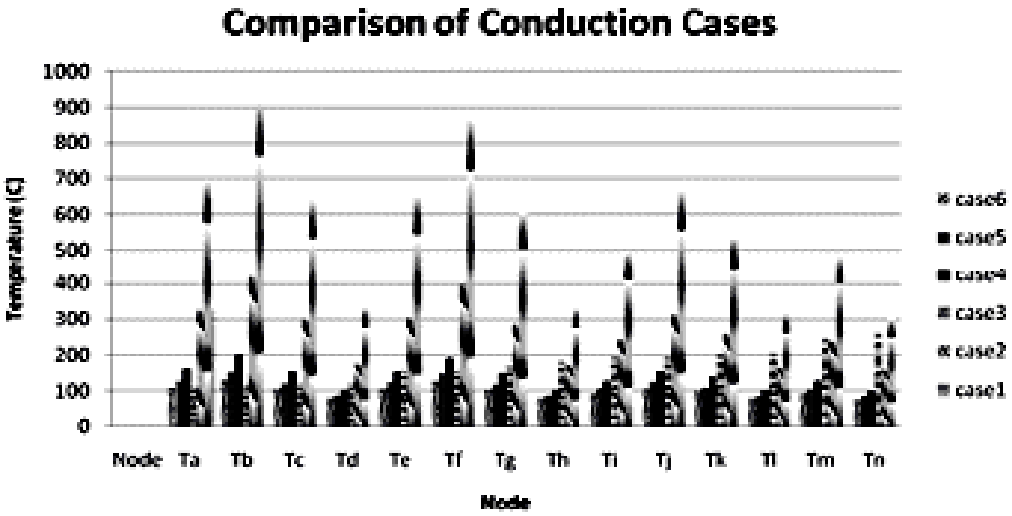

Fig. 3 Trend of reduction in nodal temperatures and comparison of conduction cases

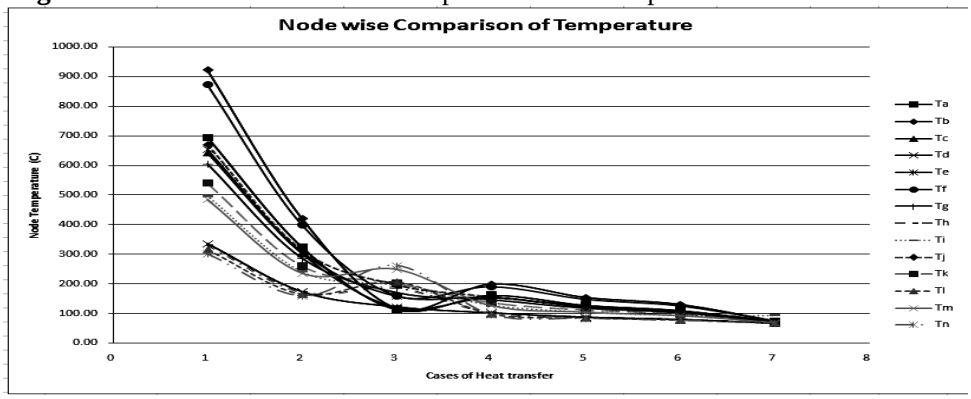

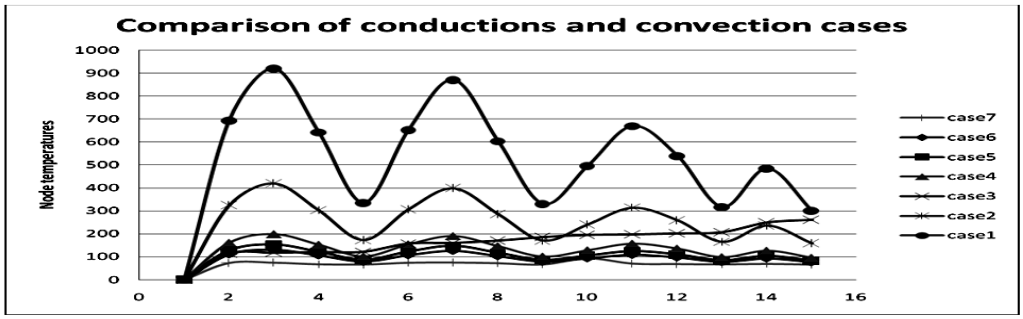

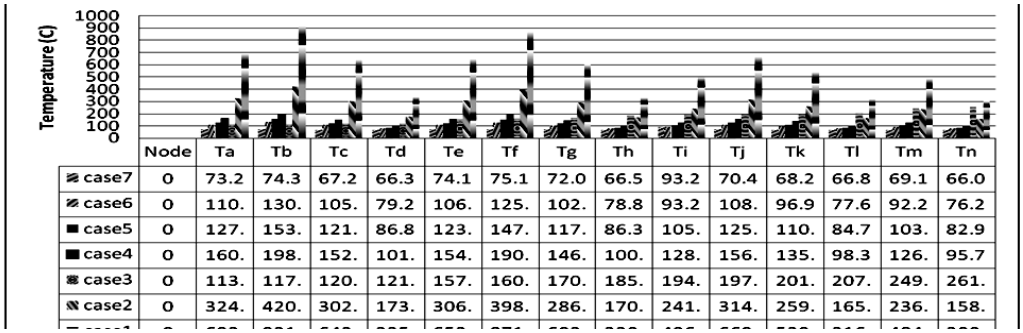

	Node	Ta	Tb	Tc	Td	Te	Tf	Tg	Th	Ti	Tj	Tk	Tl	Tm	Tn
case7	0	73.2	74.3	67.2	66.3	74.1	75.1	72.0	66.5	93.2	70.4	68.2	66.8	69.1	66.0
case6	0	110.	130.	105.	79.2	106.	125.	102.	78.8	93.2	108.	96.9	77.6	92.2	76.2
case5	0	127.	153.	121.	86.8	123.	147.	117.	86.3	105.	125.	110.	84.7	103.	82.9
case4	0	160.	198.	152.	101.	154.	190.	146.	100.	128.	156.	135.	98.3	126.	95.7
case3	0	113.	117.	120.	121.	157.	160.	170.	185.	194.	197.	201.	207.	249.	261.
case2	0	324.	420.	302.	173.	306.	398.	286.	170.	241.	314.	259.	165.	236.	158.

Fig. 4 Node wise comparisons of Temperatures

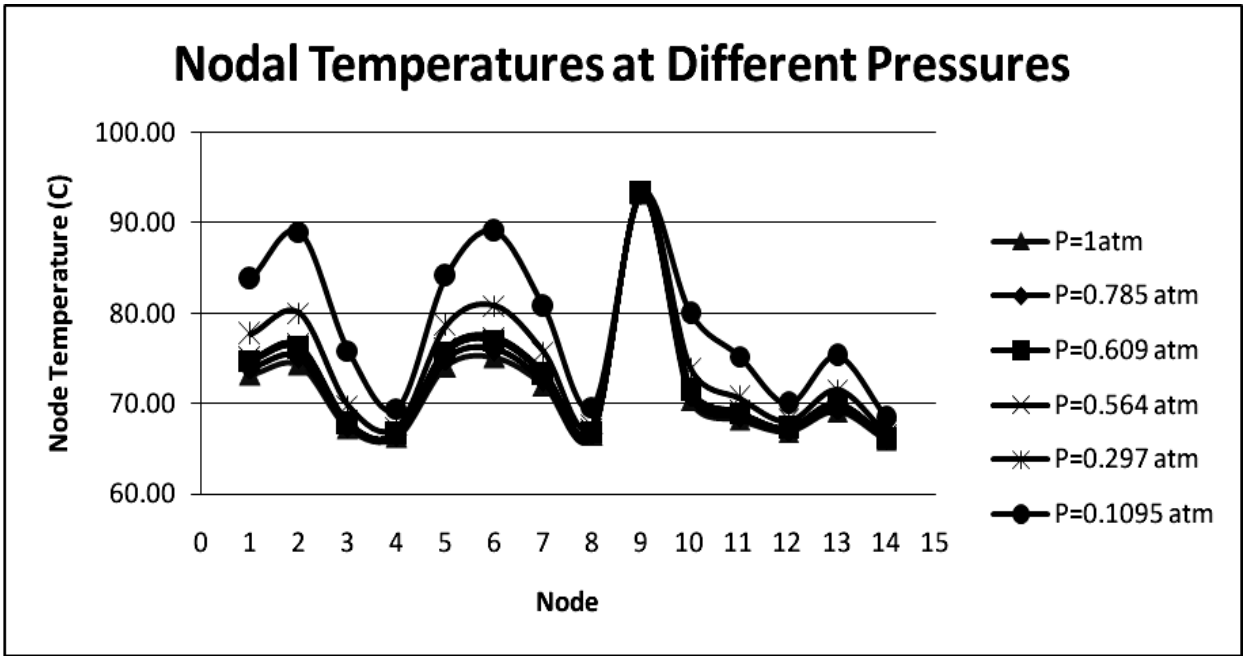

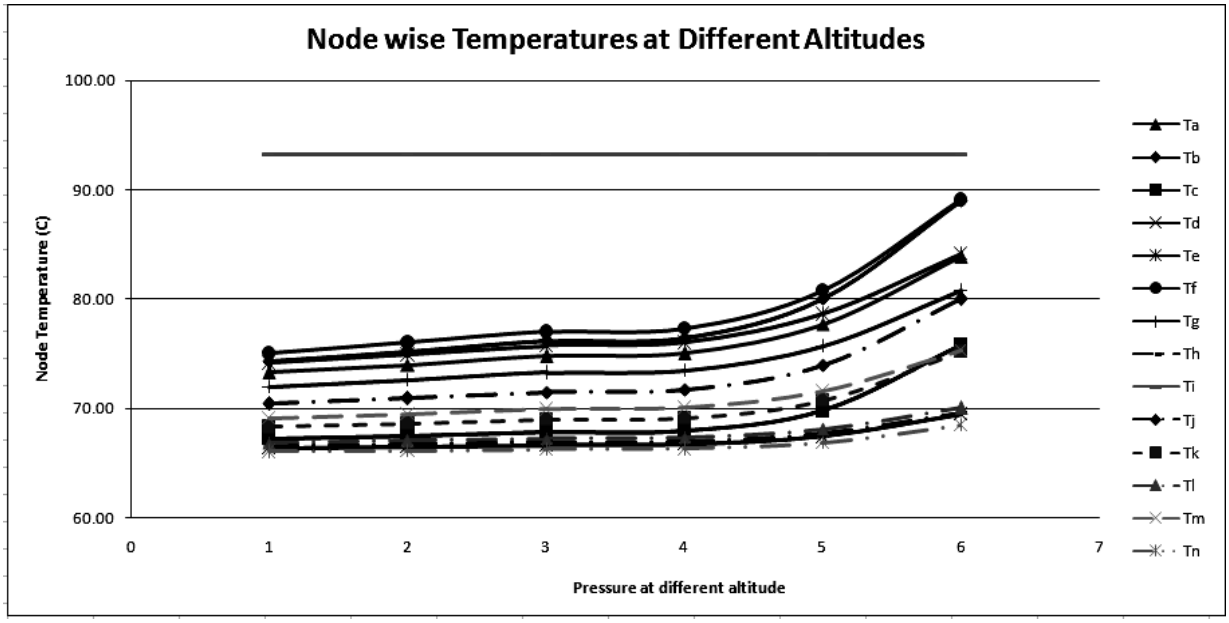

Fig. 5 Node wise temperatures at different pressures and altitudes

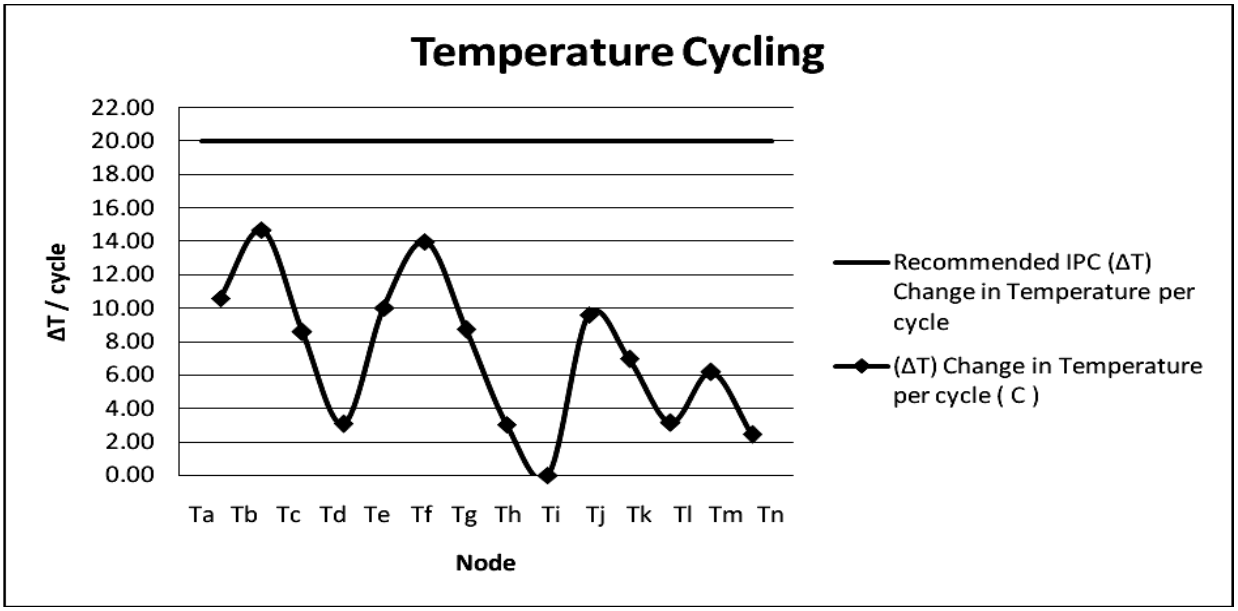

Fig. 6 Temperature cycling of electronic equipment with variation in elevation

5. Conclusions

Current work is focused on the thermal analysis of electronic equipment suitable to be installed in an aircraft. The analysis of electronic equipment provides the maximum permitted temperatures of the electronic components. Following are the important findings of the study:

- It is found that temperatures of all critical electronic components are within the derated values and that the slight increase in the copper percentage causes a significant increase in the effective thermal conductivity of PCB, and thus results in appreciable increase in the heat transfer through conduction in electronic equipment.
- It is found that convection plays a key role in the cooling of electronic equipment used in aircrafts, and hence maintains them within safe and reliable ranges of operating temperature.
- The variation in altitude from sea level to 15240 m above sea level with corresponding change in pressure from 1 atm to 0.1095 atm causes the rise in the temperature of the electronic components from 73.25^{o}C to 83.83^{o}C; for a certain node, owing to the reduction in the convective heat transfer coefficient.
- It is finally confirmed that as the altitude of the aircraft changes, the temperatures of the electronic components during the thermal cycling remain within the range as recommended by IPC.

6. References

[1] Y.A. Cengel, "Heat Transfer: A Practical Approach", Second Edition, McGraw-Hill, 2003.

[2] T.Y. Lee, B. Chambers, M. Mahalingam, "Application of CFD technology to electronics thermal management", Components, Packaging, and Manufacturing Technology, Part B: Advanced Packaging IEEE, Vol. 18, Issue: 3, pp. 511 – 520, August 1995.

[3] K. Ramakrishna, T.Y. Lee, J. Hause, B. Chambers, and M. Mahalinguam, "Experimental evaluation of thermal performance and cooling enhancements to a handheld portable electronic system, in process, enhanced and multiphase heat transfer", A Festschrift for A. E. Bergles, Proc. of an A. E. Bergles Symposium held at Georgia Institute of Technology, Atlanta, pp. 217-226, Begell House, Inc., New York, NY, 1997.

[4] J.R. Culham, M.M. Yovanovich, "Non-Iterative technique for computing temperature distributions in flat plates with distributed sources and convective cooling", ASME/JSME Thermal Engineering Joint Conference, Honolulu, HI, Vol. 3, pp. 403-409, 1987.

[5] M. Arik, S. Brzozowski, M. Nagulapally, and J. Glaser, "Thermal design and optimization of harsh environment power electronics in natural convection heat transfer", ASME Summer Heat Transfer Conference, HT2003-47015, Las Vegas, Nevada, 2003.

[6] V. Eveloy, P. Rodgers, M.S.J. Hashmi, "Numerical heat transfer predictive accuracy for an in-line array of board- mounted plastic quad flat back components in free convection", Journal of Electronic Packaging, Vol. 127, Issue: 3, pp. 245-254, 2004.

[7] K.J. Negus, M.M.Yovanovich, "Thermal analysis and optimization of convectively cooled microelectronic circuit boards", AIAA/ASME 4th Thermophysics and Heat Transfer Conference, Boston, Vol. 57, pp. 167-176, 1986.

[8] F. Sarvar, D.C. Whalley, "Thermal design of high power semiconductor packages for aircraft systems", Journal of Electronics Manufacturing, Vol. 9, Issue: 4, pp. 269-274, 1999.

[9] A. Jamnia, M. Dekker, "Practical guide to the packaging of electronics, thermal and mechanical design and analysis", Second Edition CRC Press, 2008.

[10] D.S. Steinberg, "Cooling Techniques for Electronic Equipment" Second Edition New York: John Wiley & Sons, 1991.

[11] E. Kreyszing, "Advanced Engineering Mathematics" Eighth Edition New York: John Wiley & Sons, 1999.

[12] S.A. Bhatti, N.A.Bhatti, "A first course in Numerical Analysis with C++", Fourth Edition, May 2002

Annexure-I

Equipment Components Details:

The details from the data sheets of the components mounted on PCB are as follows:

- **DC to DC converter**

Identification code:	MGDS-20-H-E
Quantity:	01
Manufacturer:	GAIA
Input voltage range:	9-36V
Output voltage	12V
Efficiency:	84%
Operating temperature range case:	-40 to 105^{o}C
Operating temperature range ambient:	-40 to 85^{o}C
Output current:	1600mA
Wattage capacity:	20 W
Dimensions (length-width-height) mm:	50x50x12.7
Surface area (mm^2)	5040
Power input:	16.8
Thermal Resistance case to ambient:	7C/W
Material:	Case-Metallic black paint coated

- **Resistors**

Identification code:	CBT-25-J-100
Quantity:	12
Manufacturer:	TYCO ELECTRONICS
Resistance:	100 ohm
Tolerance:	5%
Input current:	50mA
Wattage capacity:	0.25 W
Efficiency:	95%
Operating temperature range case:	-55 to 125^{o}C
Dimensions (length-width-height) mm:	43.24x11.74x2.5
Surface area (mm^2)	765.8
Power input:	0.24
Thermal resistance Junction to Case:	1.75C/W
Material:	Cu Alloy

- **Comparator**

Identification code:	LM139 Molded dip
Quantity:	01
Manufacturer:	National Semiconductors
Voltage range:	2-36V
Input current:	50mA
Wattage capacity:	1050 mW
Storage temperature range:	-65 to 150 ^{o} C
Operating temperature range:	-55 to 125 ^{o} C
Efficiency:	90%
Dimensions (length-width-height) mm:	19.34x10x9
Surface area (mm^2)	721.5
Power input:	0.95
Thermal Resistance case to ambient:	95 C/W
Material:	Ceramic Dual in line package

- **Comparator**

Identification code:	LM139 Molded dip
Quantity:	01
Manufacturer:	National Semiconductors
Voltage range:	2-36V
Input current:	50mA
Wattage capacity:	1050 mW
Storage temperature range:	-65 to 150 ^{o} C
Operating temperature range:	-55 to 125 ^{o} C
Efficiency:	90%
Dimensions (length-width-height) mm:	19.34x10x9
Surface area (mm^2)	721.5
Power input:	0.95
Thermal Resistance case to ambient:	95 C/W
Material:	Ceramic Dual in line package

- **Peripheral driver**

Identification code:	ULN2003
Quantity:	01
Manufacturer:	Texas Instruments
Output Voltage:	50V
Input current:	50mA
Wattage capacity:	0.9 W
Operating temperature range:	-25 to 95 ^{o} C
Efficiency:	92%
Dimensions (length-width-height) mm:	20.26x10.06x8
Surface area (mm^2)	688.9
Power input:	0.83

- **Octal bus transceiver**

Identification code:	74LS245
Quantity:	01
Manufacturer:	National Semiconductors
Input Voltage:	7 V
Input current:	24mA
Wattage capacity:	1.2375 W
Operating temperature range:	-65 to 150 ^{o} C
Efficiency:	82%
Dimensions (length-width-height) mm:	25.45x10.12x8
Surface area (mm^2)	826.7
Power input:	1.014

- **Male connector**

Identification code:	37 pin D-type
Quantity:	01
Dimensions (length-width-height) mm:	69.24x20.90

- **Electrolytic capacitor**

Identification code:	470 µF -16Volt
Quantity:	01
Manufacturer:	SGS- Thomson Microelectronics
Input Voltage:	16 V
Input current:	24mA

Wattage capacity:	0.06 W
Operating temperature range:	-40 to 85 ^{o}C
Efficiency:	96%
Dimensions (length-width-height) mm:	16.85x23.27x9.4
Surface area (mm^2)	734.2
Power input:	0.057

- **Diode**

Identification code:	IN4148
Quantity:	1
Manufacturer:	SGS- Thomson Microelectronics
Input Voltage:	5 V
Input current:	30mA
Wattage capacity:	0.05 W
Storage temperature range:	-65 to 150 ^{o} C
Operating temperature range:	0 to 80 ^{o}C
Efficiency:	94%
Dimensions (length-width-height) mm:	10.58x20.47x1.57
Surface area (mm^2)	145.9
Power input:	0.28
Material:	Carbon, lead of Cu

- **Resistors**

Identification code:	47 ohm-1/4watt-5% Tolerance
Quantity:	4
Manufacturer:	Texas Instruments
Resistance:	47 ohm
Tolerance:	5%
Input current:	7.5 mA
Wattage capacity:	0.25 W
Operating temperature range:	-55 to 125^{o}C
Efficiency:	96%
Dimensions (length-width-height) mm:	28.76x11.68X2.5
Surface area (mm^2)	255.3
Power input:	0.24

Solder tinned Cu alloy, Substrate-96% Alumina

- **Resistors & Relay**

Identification code:	560 ohm-1/4Watt-5% Tolerance
Quantity:	4
Identification code:	24 ohm-1/4Watt-5% Tolerance
Quantity:	4
Manufacturer:	Texas Instruments
Resistance:	24 ohm
Tolerance:	5%
Input current:	288mA
Wattage capacity:	3.37 W
Identification code of Relay:	M39016-28V
Quantity:	4
Manufacturer:	KKI microelectronics
Resistance:	700 ohm
Input Voltage:	28 V
Input current:	0.15 A

Wattage capacity:	3.37 W
Operating temperature range:	-25 to 125^{o}C
Efficiency:	80%
Dimensions (length-width-height) mm:	21x21x3.46
Surface area (mm^2)	1096.5
Power input:	0.674
package CBGAFC-21x21x2R	

- **Paper capacitor**

Identification code:	331-330 µF
Quantity:	04
Manufacturer:	SGS- Thomson Microelectronics
Input Voltage:	16 V
Input current:	24mA
Wattage capacity:	0.042 W
Operating temperature range:	-40 to 85 ^{o}C
Efficiency:	96%
Dimensions (length-width-height) mm:	7.03x20.57x5
Surface area (mm^2)	157
Power input:	0.04

- **Paper capacitor**

Identification code:	104-0.1µF
Quantity:	02
Manufacturer:	SGS- Thomson Microelectronics
Input Voltage:	16 V
Input current:	24mA
Wattage capacity:	0.042 W
Operating temperature range:	-40 to 85 ^{o}C
Efficiency:	96%
Dimensions (length-width-height) mm:	7.46x8.37x5
Surface area (mm^2)	78.53
Power input:	0.04